J. Fluid Mech. (1966), *vol.* 26, *part* 2, *pp.* 321–336
Printed in Great Britain

The structure of the wave front in spinning detonation

By D. H. EDWARDS, D. J. PARRY AND A. T. JONES
Department of Physics, University College, Aberystwyth

(Received 6 May 1965 and in revised form 10 December 1965)

The structure and mode of propagation of spinning detonation waves in stoichiometric oxyhydrogen, at initial pressures of 20–30 mm, have been investigated. The waves were generated in a square-section tube and observations have been made by the smoked-film technique, spark schlieren photography and pressure gauges. At the front of the self-sustaining detonation waves obtained at these pressures, two Mach interactions exist, the trajectories of which are derived from the imprints made on the smoked foil. As the triple point traverses the tube section, its direction of motion is found to vary between 50° and 70° with the tube diameter. An analysis of a Mach triple point for these conditions predicts the absence of chemical reaction behind the Mach stem in the immediate neighbourhood of the triple point. Experimentally determined pressures and triple shock angles confirm, to within experimental error, the postulated theoretical configuration.

1. Introduction

The existence of periodic disturbances in detonation waves propagating in tubes, termed spinning waves, has been known for some forty years. These disturbances have a transverse structure comparable with the tube diameter and were found to occur in gaseous mixtures near the limits of detonability and also as a transient process during the decay of over-driven waves in mixtures incapable of supporting a self-sustaining detonation. The phenomenon appears to have been discovered by Campbell & Woodhead (1926) when making photographic studies of detonation waves in cylindrical tubes. Other notable early work is that of Bone & Fraser (1929) and Bone, Fraser & Wheeler (1936) with carbon monoxide–oxygen mixtures. These observations were made by recording the progress of a detonation wave by means of a streak camera in which the photographic film moves at right angles to the direction of travel of the detonation wave in the tube. If the waves had been one-dimensional, then a straight inclined track, corresponding to the head of the detonation wave, would have been recorded. In these mixtures, however, a sinusoidal track was obtained with striations appearing in the burnt gas region behind the front. By taking a 'head-on' photograph of one of these waves Campbell & Finch (1928) demonstrated that a highly luminous zone, occupying only a fraction of the tube cross-section, rotates around the tube axis along the tube surface, as the detonation travels along the tube. This spiralling or spinning head caused a helical track to

be cut in the walls of a glass tube which had been silvered on the inside (Bone *et al.* 1936).

Earlier efforts to explain this phenomenon were largely qualitative and an arbitrary distinction was recognized between waves exhibiting this feature and the 'non-spinning' waves which belonged to the more highly exothermic mixture compositions. The first significant contribution to its understanding was made independently by Manson (1947) and Fay (1952). As the periodicity of the disturbances behind the detonation front was observed to be dependent on both the cross-sectional dimension of the tube and the speed of sound in the burnt gas, these authors were able to show that the observed frequencies are consistent with the presence of a transverse pressure oscillation in the wake of the front. Any non-uniformity of energy release at the front will give rise to pressure disturbances which themselves will react on the front and modulate the reaction rates through the ensuing temperature variations. A maintained system is thus established in which part of the energy of reaction is dissipated in the oscillatory motion. Acoustic theory is employed in the analysis and although fairly large pressure amplitudes can occur in the oscillations, the frequencies predicted by the theory are in close agreement with observed values, which vindicates its essential correctness. The success of the theory, however, does not depend upon a detailed description of the interaction of the oscillation with the detonation front. Clearly, such an interaction implies a departure from the one-dimensional Chapman–Jouguet (C–J) model which visualizes the reaction zone and the following non-steady expansion as quasi-independent régimes.

In the subsequent development of our ideas of the wave-front structure in spinning waves, notable contributions have been made by Denisov & Troshin (1962) and Duff (1961). These authors employ the smoked-film technique which reveals diamond-shaped patterns arising from wave interaction with the tube wall. A characteristic feature of a spinning wave is a highly non-planar wave front in which the causal shock is curved and exhibits one or more irregularities or 'breaks'. These 'breaks' move transversely to the direction of wave propagation and have been identified as Mach interactions. In general, when non-reactive shock waves are diffracted, Mach reflexions occur, and these tend to reduce the influence of the diffracting perturbation and restore one-dimensional flow. Duff argues, by analogy to this shock-diffraction process, that the Mach interactions in spinning detonation waves attempt to minimize the disturbance caused by the instability of the reactive flow behind the causal shock. A Mach interaction comprises three shocks, the incident, reflected and Mach stem, and a slip stream, all of which meet at a triple point. When a triple point interacts with a smoked-film placed on the inside wall of the detonation tube, a line is scored which gives the locus of the trajectory of the triple point at the wall. Denisov & Troshin interpret a single Mach interaction as being the criterion for a spinning wave as envisaged by the theories of Manson and Fay, whereas the presence of two or more triple points at the wave front is assumed to require a different mode of propagation, which they term 'pulsating'. On the other hand, Duff rejects this postulation and argues that the characteristic diamond patterns are explained by the helical progress of Mach triple points along the wall of a circular tube in both clockwise

and anti-clockwise senses. Further considerable progress in the elucidation of the structure of the Mach interactions, has resulted from the outstanding work of White (1963). This author employs a two-dimensional nozzle in a square-section tube to overdrive a detonation wave, which, as its velocity decays, develops a single Mach interaction the progress of which is recorded by a high-speed spark interferometer. Strehlow (1964) has analysed the Mach stems observed by White and shown that the experimental angles are in agreement with the values calculated under the assumption that no chemical reaction occurs in the immediate vicinity of the triple point.

In the present work self-sustaining detonation waves in oxyhydrogen mixtures are examined in order to test and provide further information on the currently held views of the wave-front structure in spinning waves. Waves with the lowest-order interaction are generated in a square-section tube and observations obtained by the smoked-film technique, spark schlieren photography and pressure gauges are described.

2. The structure of the Mach triple point

In their analysis of spinning and 'pulsating' detonation Denisov & Troshin (1962) consider the conditions under which chemical reaction may occur in the immediate vicinity of the triple-points which they observe experimentally. Since this simple analysis, in which the existence of finite induction delays is ignored, is relevant to our present observations, it is briefly outlined. The incident shock, Mach stem, slip surface and reflected shock are represented by OI, OM, OS and OR respectively in figure 1 and the various gas stages are defined by the numbers shown. A large induction zone is assumed to exist behind OI. A frame of reference is chosen which brings the triple point O to rest. Consequently if χ is the angle which the motion of O makes with a normal to the tube axis then, in this frame of reference, this is also the angle at which the effective incident flow will meet the incident shock OI. This follows because the motion of this shock is axial and has no transverse component of velocity. If D denotes the velocity of the incident shock wave, which is not, in general, the C–J velocity, then the effective Mach number of the incident flow with respect to the triple point is $M_1 = D/(a_1 \sin\chi)$, where a_1 is the velocity of sound in the unreacted gas. The Mach stem is, therefore, an over-driven wave in which the combustion delay is short. For OM the energy equation may be written in the form

$$(1+q)h_1 + \tfrac{1}{2}u_1^2 = h_4 + \tfrac{1}{2}u_4^2, \tag{1}$$

where h_1 and h_4 are the specific enthalpies, u_1 and u_4 the flow velocities in states 1 and 4 respectively and $q = Q/h_1$, where Q is the effective heat release per gram of mixture during reaction. For a calorically perfect gas, equation (1) becomes

$$(1+q)\frac{2\gamma_1}{\gamma_1 - 1}\frac{p_1}{\rho_1} + u_1^2 = \frac{2\gamma_4}{(\gamma_4 - 1)}\frac{p_4}{\rho_4} + u_4^2. \tag{2}$$

Eliminating u_1 and u_4 by using equation (2) and the mass- and momentum-conservation equations across the Mach stem, gives

$$\frac{\rho_1}{\rho_4} = \frac{p_{41} + (1+q)m_1}{m_4(1+p_{41}) - p_{41}}, \tag{3}$$

where $m = 2\gamma/(\gamma-1)$, and $p_{41} = (p_4-p_1)/p_1$. If β denotes the angle which OM makes with the incident flow and η the deviation of the flow produced by OM, then from the usual oblique-shock relations it follows that

$$\tan\eta = \frac{\sin\beta\cos\beta\,(1-\rho_1/\rho_4)}{1-\sin^2\beta(1-\rho_1/\rho_4)}. \tag{4}$$

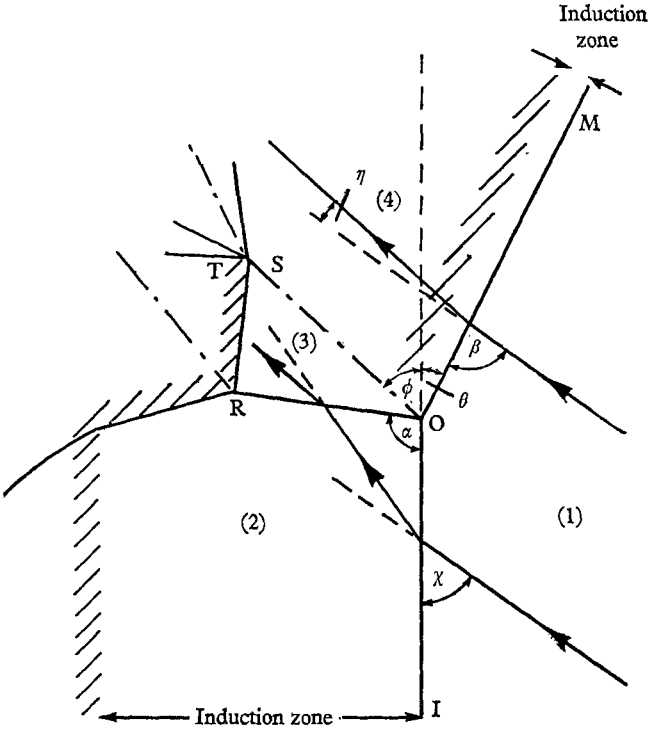

FIGURE 1. Schematic diagram of a Mach interaction describing the symbols used in the text. Triple point, O; Mach stem, OM; incident shock, OI; reflected shock, OR; slip stream, OS; reaction shock, RT. Hatching indicates onset of combustion.

Furthermore, the pressure ratio p_{41} across an oblique shock, inclined at an angle β to the incident flow M_1, is given by (Liepmann & Roshko 1960)

$$p_{41} = \gamma_1 M_1^2 \sin^2\beta\{1-(\rho_1/\rho_4)\}. \tag{5}$$

Thus equations (3), (4) and (5) define the relationship between p_{41} and η for given values of M_1 and q. Moreover, by making q zero and $\gamma_1 = \gamma_4$, the above three equations reduce to those for the case of an oblique shock wave without reaction. Thus

$$\tan\eta = \frac{p_{41}}{\gamma_1 M_1^2 - p_{41}}\left(\frac{M_1^2}{[p_{41}/(\mu^2+1)]+1}-1\right)^{\frac{1}{2}}, \tag{6}$$

where $$\mu^2 = (\gamma_1-1)/(\gamma_1+1).$$

Equations (3), (4), (5) and (6) have been solved by means of a digital computer for a range of values of M_1 for the case of stoichiometric oxyhydrogen at an initial pressure p_1 of 30 torr. Thus, for the case of the Mach stem, a family of (p, η) curves

or polars can be derived, for both shock and detonation conditions, by varying the value of M_1. For a given explosive mixture and initial pressure, the values of both D and a_1 are kept constant whilst the angle χ is varied, since experimentally this angle is found to depend upon the position of the triple point with respect to the tube. In the present work the observed values of M_1 are found to lie between 4·3 and 5·9. One set of computed polars, for a value of M_1 of 5·3, is given in

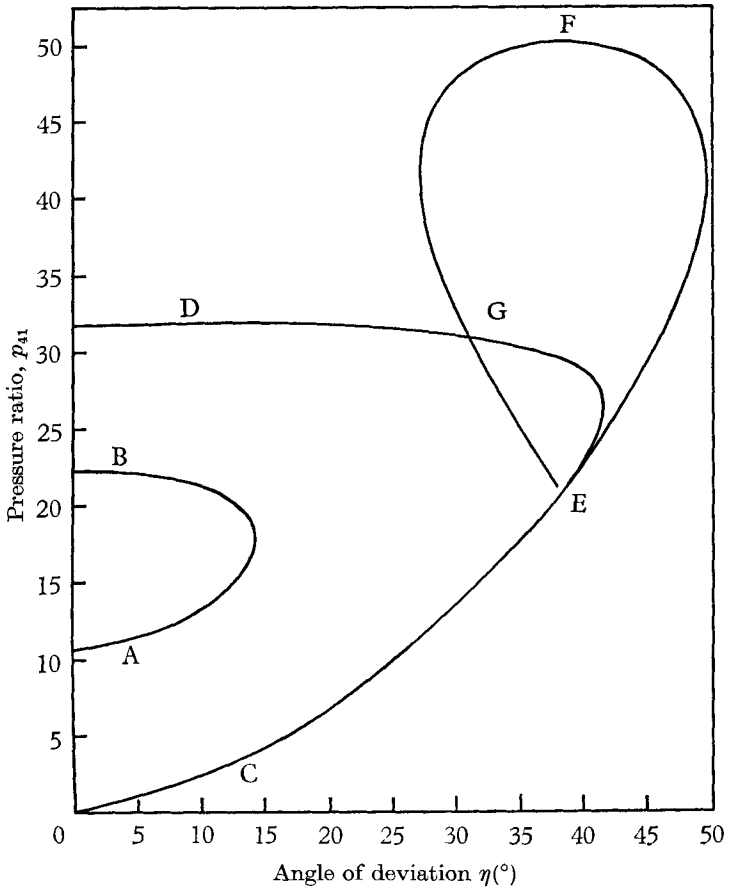

FIGURE 2. Calculated polar diagram for $2H_2+O_2$ at 30 mm initial pressure and M_1 of 5·3. Curves AB and CD refer to the Mach stem with and without chemical reaction respectively. Point E represents the pressure ratio across the incident shock, p_{21}, and curve EF is the polar of the reflected shock in the absence of reaction.

figure 2, in which the curves AB and CD represent the relation across the Mach stem with and without chemical reaction respectively. In each case the complete curves represent a variation of angle β from 0° to 90°, where these extreme values correspond to positions of zero deviation. Consequently, a unique point E can be located on curve CD where $\beta = \chi$, which physically represents the state of the gas flow behind the incident shock.

A third polar EF corresponding to the reflected shock, can now be calculated

with the point E as origin and using the flow Mach number appropriate to region 2. This is given by

$$M_2 = \frac{2+(\gamma_2-1)M_1^2}{2\gamma_2 M_1^2 \sin^2\chi-(\gamma_2-1)} + \frac{2M_1^2\cos^2\chi}{2+(\gamma_2-1)M_1^2\sin^2\chi}. \tag{7}$$

For a stable configuration two conditions must be satisfied, namely, equality of pressure across the slip-stream OS so that $p_4 = p_3$ and the streamlines in regions 3 and 4 are parallel to OS. These conditions are satisfied at the point of inter-

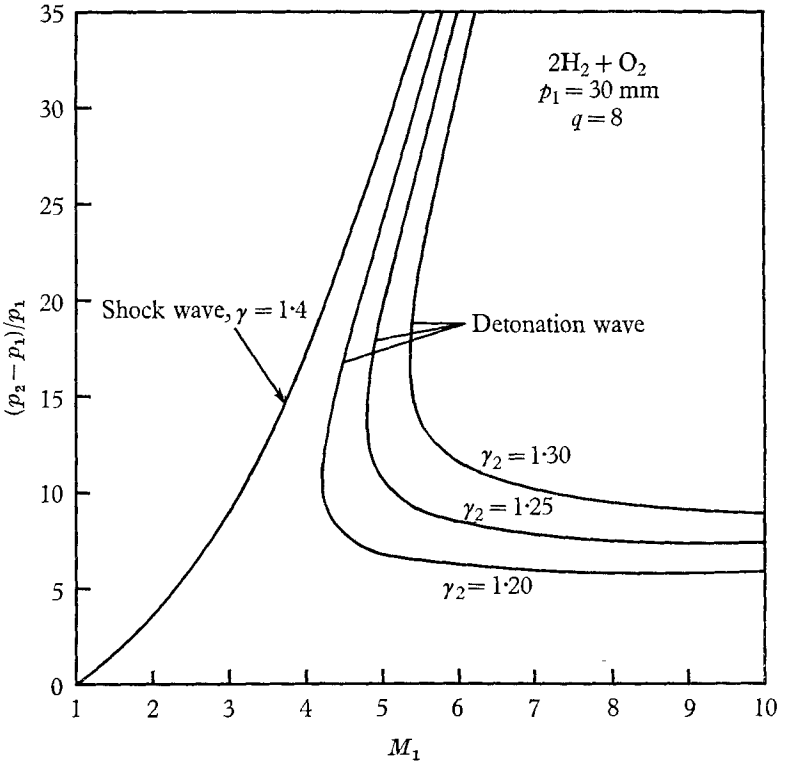

FIGURE 3. Graphs of detonation strength, $(p_2-p_1)/p_1$ against wave Mach number for a plane detonation in $2H_2+O_2$ with constant value of $q = 8$ and $\gamma_2 = 1{\cdot}20$, $1{\cdot}25$ and $1{\cdot}30$. The graph for a normal shock, $q = 0$, is shown for comparison.

section G of the two polars ED and EF. Thus the reflected shock gives a negative deviation to the flow behind the incident shock wave. This is so because β is greater than χ ($\beta = \theta+\chi$) and the flows in regions 3 and 4 are parallel; these conditions require that the flow deviation across OI is always greater than that across OM.

In the situation depicted in figure 2, for a value of M_1 of 5·3, no intersection occurs of the shock polar EF and the detonation polar AB. Consequently, no solution can be found for which reaction occurs behind the Mach stem in the immediate neighbourhood of the triple point. Moreover, the same result is found for the range of values of M_1 encountered in oxyhydrogen mixtures. It must be emphasized that this conclusion is based on the idealized assumption of the

absence of an induction zone for the reaction, in the calculation of the detonation polar AB. Clearly, since no account is taken of the kinetics of the reaction, the analysis does not purport to offer any evidence on the position of the reaction zone behind the Mach stem, but merely shows that the geometrical configuration of the Mach interaction, at any observed value of M_1, is consistent with the absence of heat release in the immediate vicinity of the triple point. This result is in agreement with the analysis of Strehlow (1964), which is discussed below, but is at variance with the conclusion of Denisov & Troshin (1962) for this mixture. However, the polars derived by the latter authors appear to be in error through their assumption of a constant value of γ following reaction. An exact calculation shows that the correct value of γ_4 for a value of p_1 of 30 mm, with complete reaction is 1·29 and that the pressure p_{41} is a sensitive function of q and γ. The dependence of the pressure across a detonation wave on q and γ is well illustrated for the case of a plane wave by the curves of figure 3. Hence, a full calculation, taking into account all the equilibria, is essential to establish the conditions and configuration at the triple point.

3. Experimental apparatus

The detonation tube is made of stainless steel and is of square cross-section with an internal side of $1\frac{1}{2}$ in. It is comprised of three sections: a driver, test section, and optical working section, 3, 12 and 3 ft. in length respectively. Fitted into the optical working section is a pair of windows of schlieren-quality glass 1 ft. long and $1\frac{1}{2}$ in. wide. This section is also fitted with an ionization probe to trigger the recording apparatus, and two side ports to take the pressure gauges. The tube can be evacuated to a pressure of $10\,\mu$ and the leak rate is $10\,\mu$/hr. Hydrogen and oxygen are obtained from commercial cylinders and are premixed before being admitted into the test section.

Detonation is initiated by means of a shock wave generated by bursting a suitable Melinex diaphragm, which initially separates the test and driver sections, by gradually pressurising the driver with hydrogen.

The schlieren spark photographs are obtained by means of a five-channel Cranz–Schardin argon spark-gap system designed by North (1962) of the National Physical Laboratory. The effective duration of the light source is $\frac{1}{5}\,\mu$sec, and the time interval between flashes can be pre-set to any desired value down to roughly $5\,\mu$sec. The schlieren system is a twin-mirror type employing 12 in. diameter, 8 ft. focal-length mirrors.

The pressure gauges employed are of the pressure-bar type described by Edwards, Davies & Lawrence (1964). They are of $\frac{1}{8}$ in. diameter and have a rise-time of $1{\cdot}5\,\mu$sec.

4. The smoked-film records

These records were obtained by placing three strips of Melinex film, $1\frac{1}{2}$ in. by 9 in., adjacent to each other along three internal walls of the detonation tube and securing their ends to the tube wall with sellotape. A uniform film of soot had previously been deposited on each strip by means of a turpentine or paraffin

flame. After an experiment the strips were carefully removed and sprayed with a weak solution of shellac to avoid damaging the record.

A sketch of a typical smoked-film record is given in figure 4. The initial pressure of the oxyhydrogen mixture was 25 mm and detonation was initiated by a driving pressure of 6 atmospheres of hydrogen. The single tracks, such as the one labelled AB, arise from the movement of a Mach triple point along the wall. In this

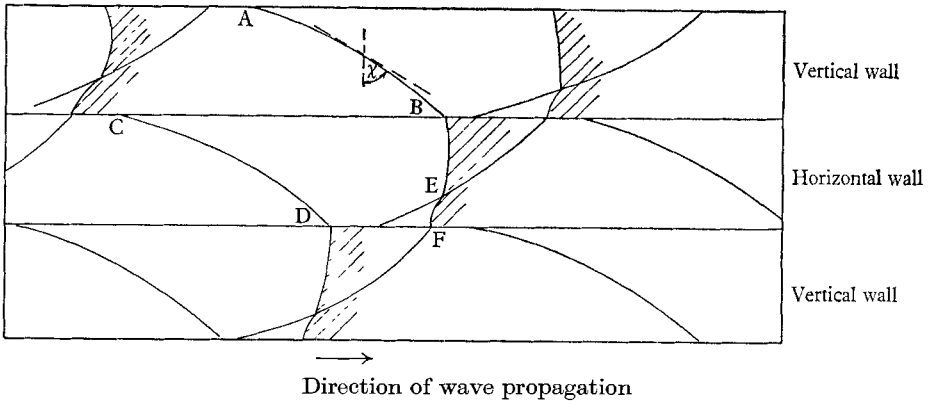

FIGURE 4. Sketch of smoked-film record obtained with $2H_2 + O_2$ at 25 mm initial pressure. Tracks such as AB and CD are trajectories of Mach triple points and BEF, etc. indicate the collision of a Mach interaction with the tube wall. Hatching shows the regions where soot is heavily scoured.

particular wave two triple points exist which are moving in directions perpendicular to each other. Thus CD represents the triple point moving along a horizontal wall of the tube at right angles to AB, and the phase difference between the motion of the two points is approximately 90°. Records are also obtained in which the directions of motion of the triple points are 180° out of phase with that of figure 4. In other respects the records are identical and occur, as would be expected, with equal probability. As the initial pressure of the detonating mixture is increased to 45 mm, two sets of triple points occur with the corresponding points of each set moving in opposite senses. The resulting pattern of tracks observed on the smoked film will thus form the characteristic diamond shapes which have been previously reported by other authors. The number of triple points increase with increasing initial pressure, which results in a finer 'cell' size of the diamond pattern. Thus the record of figure 4 shows the simplest possible mode for a self-sustaining detonation wave in a square-section tube. Moreover, if propagation is observed in a rectangular-section tube, in which one side is several times greater than the other, the same essential features are obtained in the records, the only difference being the periodicity of the motion of the triple points traversing the two sides.

When a triple point strikes the tube wall the incidence is oblique and therefore the film is marked by the differential scouring-action of the gas flow across the incident and reflected shocks and the Mach stem. The pattern obtained by the reflexion is BEF in figure 4, and the hatching indicates the regions where soot has been removed. However, the orientation of the three shocks of a triple point

cannot be inferred from the imprint left on the smoked film, because the configuration is continually changing on impact. The most important information that may be derived from the smoked-film record is the angle at which the direction of motion of the triple point moves at any instant, such as the angle χ on AB shown in figure 4. It is seen that the direction of motion varies along the whole trajectory. This is caused by variations in the velocity of the incident shock, which has a high velocity immediately after reflexion of the triple point and subsequently decelerates as the triple point moves away from the wall. Evidence of this is also found in the schlieren and pressure records.

5. The photographic records

Two sequences of flash photographs of the detonation front in stoichiometric oxyhydrogen at 30 mm initial pressure are given in figures 5 (plate 1) and 6 (plate 2). In the first series the light cut-off edge is orientated perpendicular to the tube axis whereas in the second series the edge is parallel to the axis of the detonation tube. Two images are obtained on each photograph owing to the non-planarity of the wave front in the direction of the light beam. In figure 5, density gradients along the tube axis are recorded and the period of motion of the triple point across the side of the tube is seen to be approximately 20 μsec. With the horizontal cut-off the density gradients normal to the tube axis are made visible (figure 6), in particular, the reflected shock extending backwards into the burnt gas.

From these photographs the diagrams of figure 7, which show the main features of the detonation front, have been deduced. Figure 7 (*a*) illustrates the situation when the triple point O is moving downwards. The relative magnitudes of the induction zones behind the incident shock and Mach stem are shown and these are in accord with the results obtained by White (1963) using a two-dimensional nozzle. An interesting feature of the reflected shock wave OR is its sudden change of direction at the onset of reaction behind the incident wave. This is so since the higher sound speed of the reacted gas will cause an increase in the velocity of the reflected shock as it moves into this gas. Following this region, the profile of the reflected shock becomes rather irregular, which suggests that the gas flow is turbulent. Reaction occurs behind the reflected shock and calculation of the flow Mach number in region 3, using appropriate values in equation (7), shows that the flow is slightly supersonic, with a maximum value of M_3 of 1·1, for half the period of oscillation of the triple point. That is to say, for the interval from when O is approximately at the tube centre until it collides with the wall for both upward and downward traverses. For other positions of O the flow M_3 is slightly subsonic. Evidence of the weak reaction shock, RT, may be inferred from the pressure records. In figure 7 (*b*) the conditions at reflexion are shown. The induction zone behind the Mach stem has by now widened considerably, and the velocity of the stem is decreasing at this stage. A short time after reflexion the situation is depicted in figure 7 (*c*). A new Mach stem emerges with a very short induction zone, whereas the induction region behind the incident wave is increasing as the triple point moves upwards.

The shapes of the wave front as it moves along the square-section tube are shown in figure 8. Details of the slip surfaces, the collision process at the walls and the interaction of reflected shocks, are omitted for the sake of clarity. The movement of the triple points are indicated by dotted lines and these are seen to correspond to the tracks on the smoked-film record of figure 4.

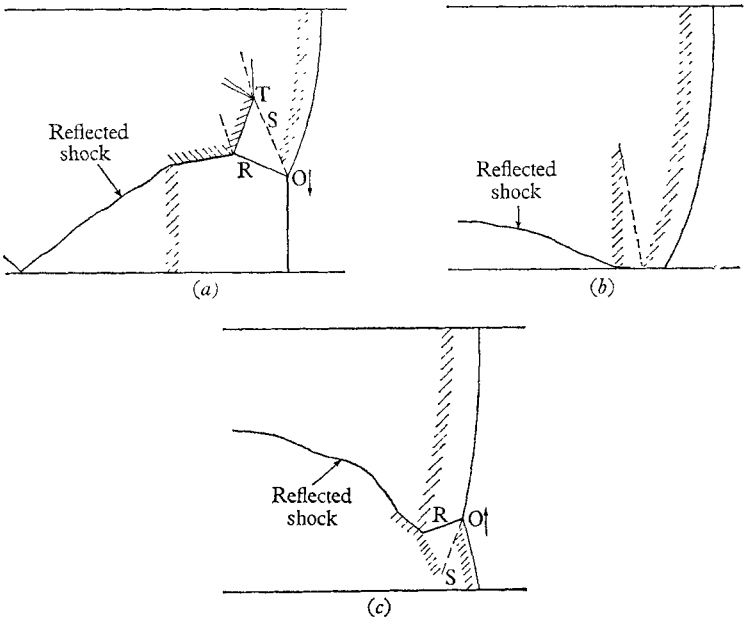

FIGURE 7. Main features of wave front deduced from photographs of figures 5 and 6: (*a*) triple point moving downwards; (*b*) collision with tube wall; (*c*) triple point moving upwards soon after reflexion.

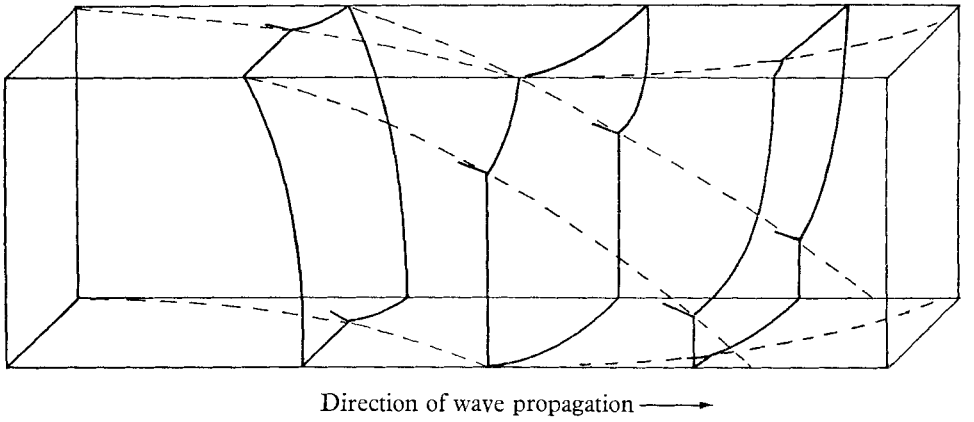

FIGURE 8. Diagram showing the wave front configuration (at three successive positions), in a self-sustaining detonation propagating in a square-section tube at low initial pressure. Dotted lines show the trajectories of the triple-points along the tube walls.

6. Pressure records

Static-pressure measurements were made by two $\frac{1}{8}$ in. diameter bar gauges mounted in the side wall of the tube near the optical windows. As the inherent rise-time of these gauges is 1·5 μsec and the traverse time of the waves across the face of the gauges is of this order, pressure changes occurring in the first 2 μsec behind the detonation front cannot be resolved. Thus, the induction zone behind the Mach stem is not observed, but a true recording of the reaction-zone pressure is obtained. Three examples of pressure records are given in figure 9 which typify the main features of the observations. In figure 9 (*a*) tracings of two records are shown to illustrate the degree of reproducibility between the two gauges. The first peak, A, occurring at 2 μsec, is the pressure in the reaction zone behind the Mach stem. A rapid fall is observed in this zone to the point B, which occurs in most records at times varying between 6 and 8 μsec. From the analysis of the wave photographs the only feasible interpretation of this 'knee' in the pressure profile is that it corresponds to the weak-reaction shock behind the reflected shock, shown in figure 7 (*a*). As the reaction proceeds, in this region the pressure continues to fall until the reflected shock sweeps past the gauge and causes the pressure to jump to point C at about 12 μsec behind the Mach stem. Thereafter the pressure remains fairly constant until the arrival of the reflected shock from the wall of the tube at a time of about 35 μsec.

If the incident shock is the first to arrive at the plane of the gauge, the type of pressure profile observed may be either that of figure 9 (*b*) or 9 (*c*), which correspond to an initial gas pressure of 30 and 20 mm respectively. In figure 9 (*b*) the peak, A, again is characterized by the absence of an observable induction zone owing to the gauge limitations and traverse time. However, the pressure knee due to the reaction shock is observed at 8 μsec. The second rise, C, at 15 μsec, with a pressure ratio of approximately two, is due to the reflected shock. This is followed by a further peak D, similar to C, arising from the reflected shock associated with the second Mach triple point and travelling at right angles to the plane of the gauge. In the record of figure 9 (*c*) an induction zone is seen to occur, following the incident shock, of 5 μsec duration. At a time of 30 μsec a large sharp-fronted peak occurs, with a pressure ratio of 37, which is caused by the collision of the two reflected shocks associated with each triple point. Most of the pressure records taken fall into one of the above three categories.

The average Mach number of the incident shock, D/a_1, in all the experiments performed at initial pressures between 20 and 30 mm, lies between 4·0 and 4·4, which is considerably below the theoretical C–J Mach number of 4·95. Moreover in any particular experiment the velocity of the incident wave is continually changing, being high immediately after the reflexion of a triple point and decelerating before the occurrence of the following reflexion. Consequently, this makes a comparison of observed and calculated pressures difficult, as can be seen from the plot shown in figure 10, in which average values of observed Mach numbers are used. The rather large scatter in measured pressure ratios for the incident shock is undoubtedly due to the deviations of the instantaneous velocities from the observed mean values. In the case of the Mach stem pressures

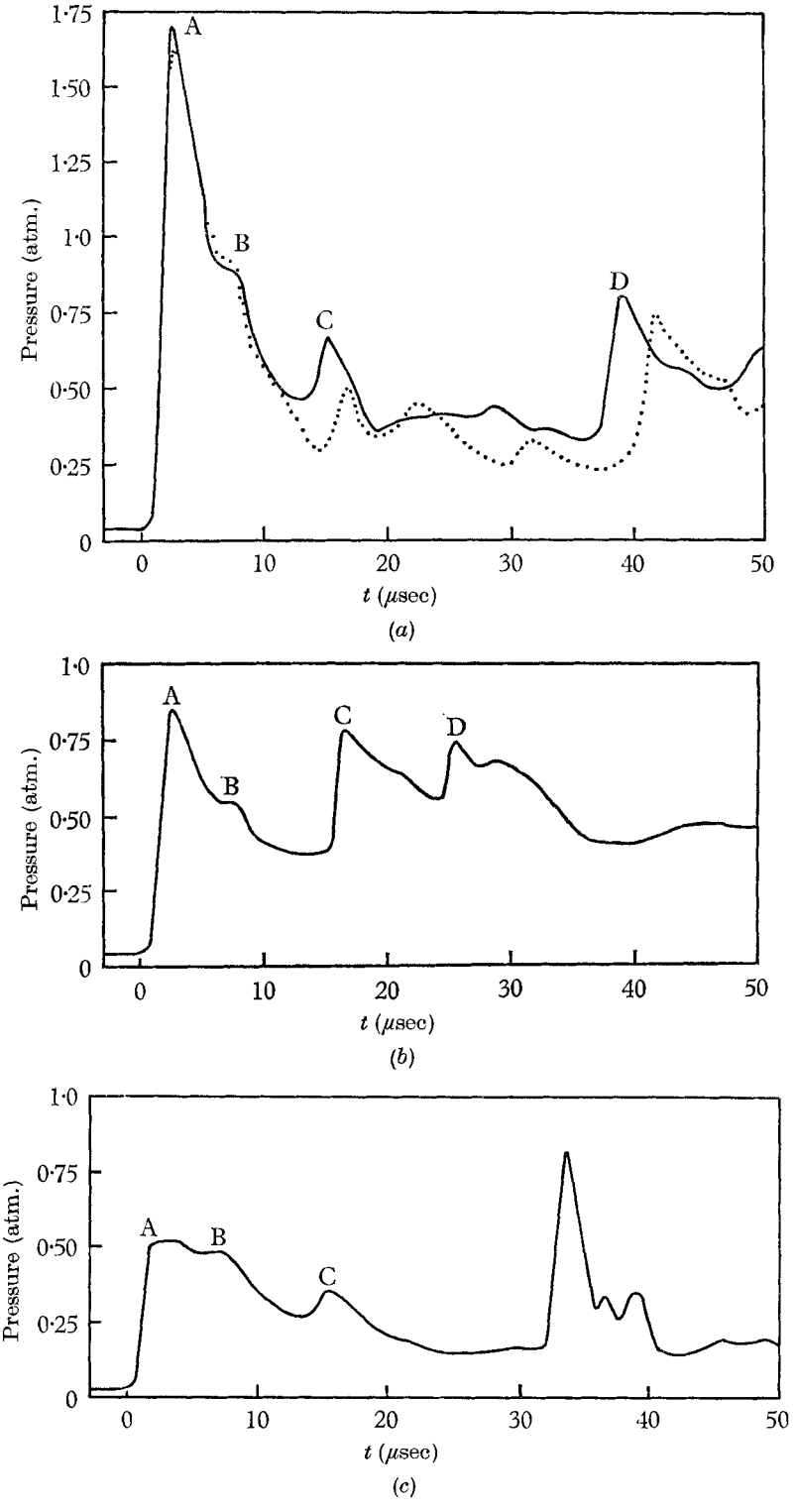

FIGURE 9. Pressure variation with observer's time for detonation wave in $2H_2 + O_2$ at initial pressures, in (*a*) and (*b*) 30 mm and (*c*) 20 mm.

a further uncertainty occurs which arises from variations in the angle χ (figure 4) which the triple point makes with the tube diameter. For the region in which the Mach stem pressures are recorded the values of χ lie between 50° and 70°; the estimated maximum error for these pressures is indicated by the horizontal lines.

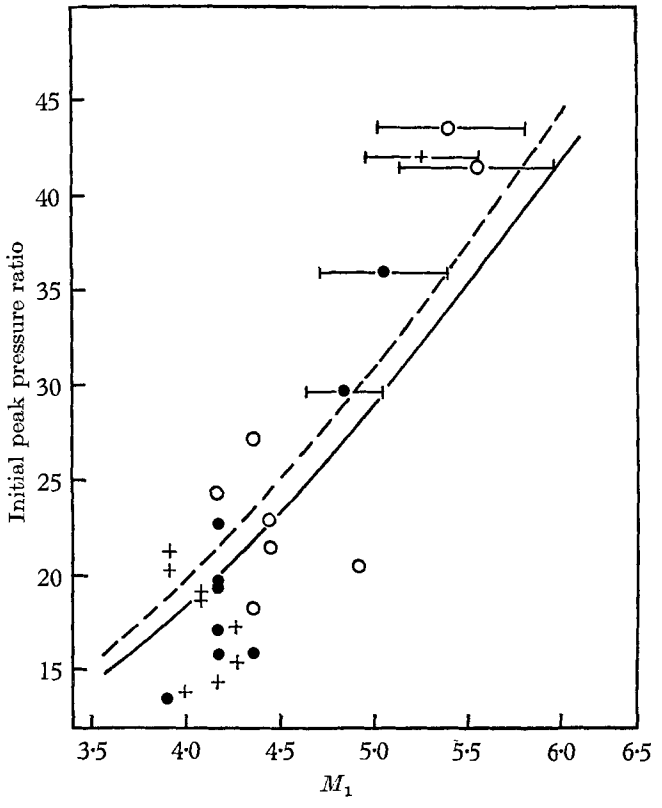

FIGURE 10. Observed peak pressure ratios vs. mean incident Mach numbers for detonation waves in $2H_2+O_2$. Initial pressures: +, 20 mm; ●, 25 mm; ○, 30 mm. Solid and broken curves are computed values for γ_2 of 7/5 and 9/7 respectively.

7. Triple shock angles

Reference has already been made to the analysis which Strehlow (1964) carried out on the Mach interactions observed by White in a detonation tube containing a two-dimensional nozzle. Excellent agreement is observed between the measured values of shock angles and those calculated under the assumption of no reaction in the vicinity of the triple point, for waves in $2H_2+O_2+2CO$. In these experiments, however, although the velocity of the detonation front is decaying continuously as it emerges from the nozzle, it can be measured with a fair degree of precision at any particular point in the tube. As already noted, this differs from the situation with self-sustaining detonation waves where the mean velocity is constant, but over short intervals is non-steady. As a result, not only do the pressure ratios across the three shocks vary, but also the geometrical configuration of the interaction. Calculated values of the angles defined in figure 1, for the

case of no reaction, are given in the curves of figures 11 and 12, for comparison with values obtained from the schlieren photographs. As in the case of the pressure results given in figure 10, although there exists a fair degree of scatter

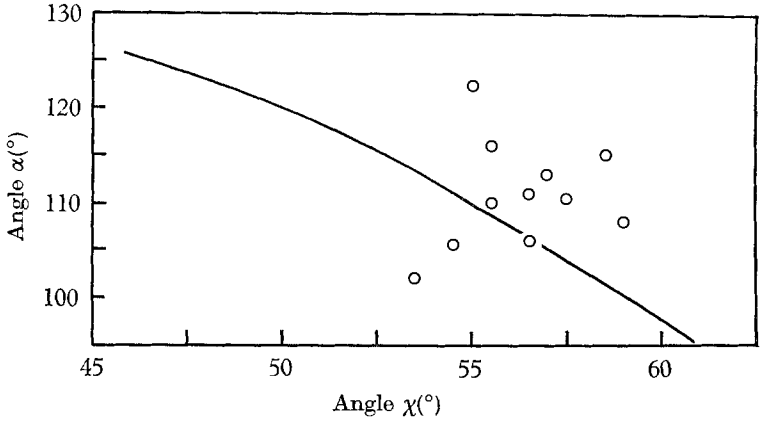

FIGURE 11. Theoretical curve and observed values of angle between incident and reflected shock, α, and angle of triple-point trajectory, χ.

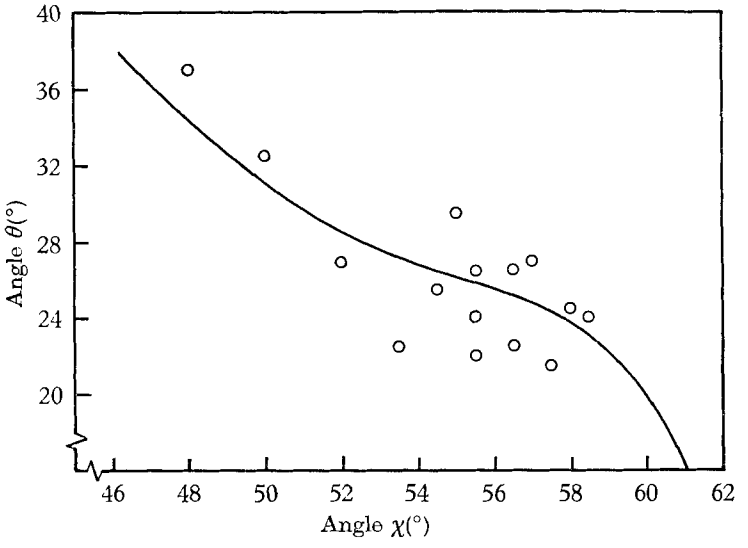

FIGURE 12. Theoretical curve and observed values of angle between Mach stem and vertical, θ, and angle of triple-point trajectory, χ.

in the measured angles, there is general agreement between theory and experiment. The calculated angle between the slipstream and the vertical, angle ϕ, remains constant at a value of 24·5° over the range of Mach numbers observed, whereas the observed value for this angle is somewhat lower, $17° \pm 2°$.

8. Conclusions

In a tube of rectangular or square section the simplest mode of propagation which is possible for a self-sustaining detonation is one that has two Mach interactions at the detonation front. For a stoichiometric oxyhydrogen mixture in a $1\frac{1}{2}$ in. square-section tube this mode occurs at initial pressures of 20 to 30 mm. As the initial pressure is increased the induction and reaction periods are reduced and the number of interactions at the front increase. Consequently, the pressure ratio across the reflected shocks is progressively weakened.

An assumption which is implicit in the comparison made between the measured pressure ratios and shock angles and their theoretical values is that the two triple points do not influence each other. In waves which have a large number of Mach interactions the pressure ratio across the transverse shocks is small so that the acoustic principle of super-position holds. However, when only two triple points are present the pressure ratio across the reflected shocks is approximately two, hence their interaction does lead to some deviation in the theoretically predicted behaviour. None the less, the nature of the observed agreement confirms that the description given of the wave front is essentially correct.

The origin of the pressure oscillation in the wake of the detonation front in spinning waves is seen to be the reflected shocks. Since the source of the reflected shocks, the triple points of the Mach interactions, move transversely to the tube axis, herein lies the reason for the transverse character of the gas oscillations required by the acoustic theory of Manson (1947) and Fay (1952).

The work described here had been completed before the publication of a paper by Schott (1965) on the structure of spinning detonation. He has studied the propagation of waves in highly diluted oxy-acetylene mixtures at low initial pressures in cylindrical tubes, using a variety of experimental methods, which include the smoked-film technique. The main structural features deduced by Schott are in broad agreement with the present observations. In particular, his most important conclusion, that reaction occurs behind the transversely propagating reflected shock, concurs with the present findings from the schlieren and pressure recordings.

The authors wish to acknowledge their indebtedness to the Director, National Physical Laboratory, and Mr R. J. North of the Aerodynamics Division, N.P.L., for the loan of the multi-channel spark light-source system employed in the present work. One of us (D. J. P.) is indebted to the D.S.I.R. for a Research Studentship.

REFERENCES

Bone, W. A., Fraser, R. P. & Wheeler, W. H. 1936 *Phil. Trans.* A, **235**, 29.

Bone, W. A. & Fraser, R. P. 1929 *Phil. Trans.* A, **228**, 197.

Campbell, C. & Finch, A. C. 1928 *J. Chem. Soc.* **131**, 2094.

Campbell, C. & Woodhead, D. W. 1926 *J. Chem. Soc.* **129**, 3010.

Denisov, Yu. N. & Troshin, Ya. K. 1962 *8th Symposium (International) on Combustion*, p. 600. Baltimore: Williams and Wilkins.

Duff, R. E. 1961 *Phys. Fluids.* **4**, 1427.

EDWARDS, D. H., DAVIES, L. & LAWRENCE, T. R. 1964. *J. Sci. Inst.* **41**, 609.

FAY, J. A. 1952 *J. Chem. Phys.* **20**, 942.

LIEPMANN, H. W. & ROSHKO, A. 1960 *Elements of Gasdynamics.* New York: John Wiley.

MANSON, N. 1947 *Propagation des Detonations et des Deflagrations dans les melanges gaseaux.* Paris: L'Office National d'etudes et de Recherches Aeronautiques.

NORTH, R. J. 1962 *N.P.L. Aero. Note* no. 1008.

SCHOTT, G. L. 1965 *Phys. Fluids*, **8**, 850.

STREHLOW, R. A. 1964 *Phys. Fluids*, **7**, 908.

WHITE, D. R. 1963 *Phys. Fluids*, **6**, 1011.

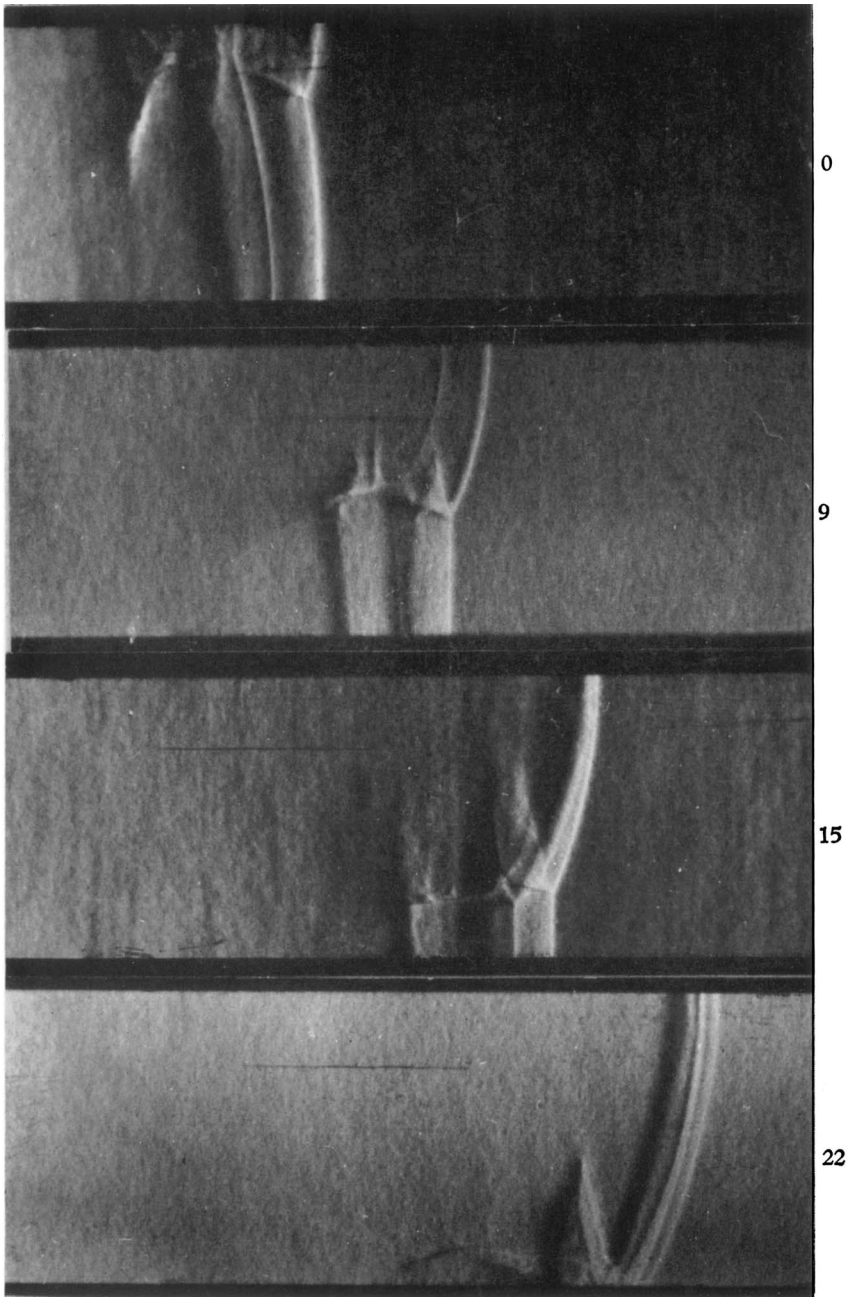

FIGURE 5. Multiple-spark schlieren photographs of detonation wave in $2H_2 + O_2$ at 30 mm initial pressure. Vertical knife-edge. Numbers denote times in μsec.

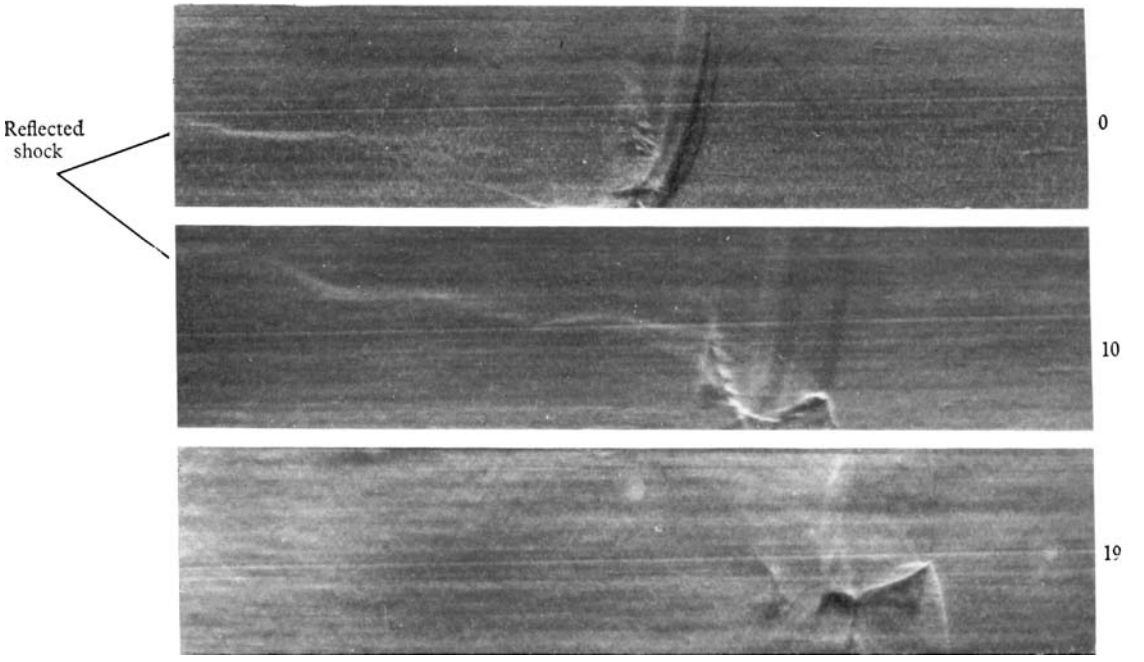

FIGURE 6. Multiple-spark schlieren photographs of detonation wave in $2H_2 + O_2$ at 30 mm initial pressure. Horizontal knife-edge. Numbers denote times in μsec.